2.6. QG POTENTIAL VORTICITY AND THE HEIGHT TENDENCY EQUATION

Applying the chain rule to carry the vertical derivative through the differential thermal advection term (term C) in (2.32), we obtain the following two terms:

$$-\frac{\partial}{\partial p}\left[\frac{f_0^2}{\sigma}\vec{V}_g\cdot\nabla\left(\frac{\partial\Phi}{\partial p}\right)\right] = -\frac{\partial\vec{V}_g}{\partial p}\cdot\nabla\left(\frac{f_0^2}{\sigma}\frac{\partial\Phi}{\partial p}\right) - \vec{V}_g\cdot\nabla\frac{\partial}{\partial p}\left(\frac{f_0^2}{\sigma}\frac{\partial\Phi}{\partial p}\right). \tag{2.35}$$

The thermal wind relation (1.45), repeated below, can be substituted in the first right-hand term in (2.35),

$$\frac{\partial\vec{V}_g}{\partial p} = \frac{1}{f_0}\hat{k}\times\nabla\frac{\partial\Phi}{\partial p}.$$

The result is the scalar product of two perpendicular vectors, and the term vanishes,

$$-\frac{\partial\vec{V}_g}{\partial p}\cdot\nabla\left(\frac{f_0^2}{\sigma}\frac{\partial\Phi}{\partial p}\right) = \frac{f_0}{\sigma}\hat{k}\times\nabla\frac{\partial\Phi}{\partial p}\cdot\nabla\frac{\partial\Phi}{\partial p} = 0. \tag{2.36}$$

Thus, returning to the height tendency equation (2.32), term C can be replaced with the rightmost term in (2.35). We can then divide (2.32) by f_0 and rearrange to obtain

$$\frac{\partial}{\partial t}\left(\frac{1}{f_0}\nabla^2\Phi + \frac{\partial}{\partial p}\left(\frac{f_0}{\sigma}\frac{\partial\Phi}{\partial p}\right) + f\right) + \vec{V}_g\cdot\nabla\left(\frac{1}{f_0}\nabla^2\Phi + \frac{\partial}{\partial p}\left(\frac{f_0}{\sigma}\frac{\partial\Phi}{\partial p}\right) + f\right) = 0. \tag{2.37}$$

Inspection of (2.37) indicates that the quantity in parentheses is *conserved* for adiabatic, frictionless, geostrophic flow. This quantity is the *quasigeostrophic potential vorticity* (QGPV), denoted as

$$q = \frac{1}{f_0}\nabla^2\Phi + f + \frac{\partial}{\partial p}\left(\frac{f_0}{\sigma}\frac{\partial\Phi}{\partial p}\right). \tag{2.38}$$

As stated above, following adiabatic, frictionless, geostrophic flow,

$$\frac{dq}{dt_g} = 0. \tag{2.39}$$

Thus, the QG height tendency equation is simply a statement of QGPV conservation. Examination of (2.38) reveals that q is the sum of the geostrophic absolute vorticity and a term involving the vertical derivative of the thickness, which is related to the static stability. There are two powerful properties of PV, each of which we will explore in more depth in chapter 4: (i) *conservation* under certain flow conditions (from 2.39) and (ii) *invertibility*. The invertibility property states that provided information about the QGPV distribution and boundary conditions, one can recover the geopotential field associated with any part of the QGPV field and from that recover the geostrophic wind and temperature (thickness) fields. One may wonder why it would be useful to recover the same quantities from which the QGPV was computed in the first place. The answer is that the QGPV can be divided into an arbitrary number of dynamically relevant pieces, for example, a local cyclonic PV anomaly associated with an upper-level trough. Then, the QGPV can be inverted in a *piecewise* manner, and the height field (and balanced flow) associated with a given QGPV feature can be uniquely identified. These two properties make PV one of the most useful and powerful dynamical tools available to meteorologists. In chapter 4, section 5.3.6, and again in chapter 7, we will explore PV applications in greater depth.

2.7. QG ENERGETICS

Another approach to atmospheric diagnosis is the study of mechanisms that control the exchange of *energy* between the environment and a given weather system. There are several different techniques for studying the mechanisms of energy transfer in the atmosphere. The study of downstream baroclinic development with Rossby wave packets can be analyzed via *local energetics*, where the instantaneous mechanisms of energy transfer are computed at specific locations. Other studies have computed volume averages around individual storm systems, or examined time-averaged contributions to energy tendency over weeks or longer. Here, we will utilize both local and volume-average approaches to understand how the configuration of upper-level trough and ridge patterns can inform us about evolving weather systems, again within the context of the QG equations.

2.7.1. Zonal averages and perturbations

A means of isolating synoptic-scale weather systems from the background flow in which they are embedded is to subtract the *zonal average* of relevant variables from the full instantaneous value. To illustrate this method, suppose that the following u wind measurements are valid for a given set of longitude points taken along fixed latitude:

u $+25\,\mathrm{m\,s^{-1}}$ $+16\,\mathrm{m\,s^{-1}}$ $+6\,\mathrm{m\,s^{-1}}$ $+9\,\mathrm{m\,s^{-1}}$ $+17\,\mathrm{m\,s^{-1}}$ $+29\,\mathrm{m\,s^{-1}}$

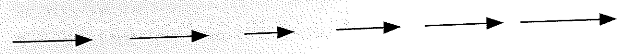

u' $+8\,\mathrm{m\,s^{-1}}$ $-1\,\mathrm{m\,s^{-1}}$ $-11\,\mathrm{m\,s^{-1}}$ $-8\,\mathrm{m\,s^{-1}}$ $0\,\mathrm{m\,s^{-1}}$ $+12\,\mathrm{m\,s^{-1}}$

These wind components can be represented as vectors, as indicated below the u values listed. Let $\bar{u}$ be the zonal average of these wind observations, and u' be the deviation from that average. At each point, $u = \bar{u} + u'$. For the data provided above, $\bar{u} = 17\ \mathrm{ms^{-1}}$, and u' is computed by subtracting this value from the point value at each location, as indicated for the lower row of values.

This simple concept can be extended to zonal averages of any meteorological variable taken around latitude circles. We will refer to deviations from the zonal average of any variable as the "disturbance," "perturbation," or "eddy" values. The total horizontal perturbation velocity ($\vec{V}' = u'\hat{i} + v'\hat{j}$) can be taken to represent the perturbation flow associated with synoptic-scale systems, such as cyclones and anticyclones. The *kinetic energy per unit mass* of the perturbation flow, or *eddy kinetic energy* (K_e) for either the full (K_e) or geostrophic (K_{eg}) flow is defined as

$$K_e = \frac{(u'^2 + v'^2)}{2}, \qquad K_{eg} = \frac{(u_g'^2 + v_g'^2)}{2}. \tag{2.40}$$

To further illustrate the process of decomposing atmospheric variables into zonal average and perturbation, Figs. 2.18 and 2.19 provide data from the GFS model for 30 September 2008. The full 500-mb geopotential height field (Fig. 2.18a) exhibits a wavy pattern of troughs and ridges; however, when the zonal mean height field (Fig. 2.18b) is subtracted, the resulting eddy height anomalies (Fig. 2.18c) appear as closed-off features. The perturbation geostrophic flow associated with these height anomalies can be computed directly from the height anomaly field, or one can simply subtract the zonal average of the horizontal wind components to determine the perturbation velocity field at each data point, as shown in Fig. 2.19. Again, in subtracting off the mean westerly flow, closed cyclonic and anticyclonic eddies become more evident.

The zero height anomaly contour or a certain kinetic energy contour can be used to define a spatial area over which to average the energy equation. Then, by integrating vertically with respect to pressure, the volume integral of geostrophic eddy kinetic energy K_{eg} over an area or disturbance is denoted $[K_{eg}]$, which is given by

$$\left[K_{eg}\right] = \frac{1}{gA}\iint\limits_{p\,A}\left(\frac{u_g'^2 + v_g'^2}{2}\right) dA\,dp. \tag{2.41}$$

The sequential downstream amplification and upstream decay of height anomalies of either sign are often associated with the eastward propagation of Rossby wave energy, as discussed in chapter 1. Viewing height anomalies, rather than the full height field, often reveals this process quite clearly.

2.7.2. The eddy kinetic energy equation

An equation for the time rate of change of K_{eg} provides insight into the growth and decay mechanisms of weather systems in terms of energy transfer processes. Given that the kinetic energy per unit mass involves terms such as u^2 and v^2, how can we form an equation that gives us the time tendency of kinetic energy (starting from the u and v momentum equations)? Taking the scalar product of the horizontal velocity vector with the horizontal momentum equation provides an equation for the time tendency of the full kinetic energy. If we instead take the scalar product of the *perturbation velocity* with the perturbation momentum equations, rather than the full equations, the following eddy kinetic energy equation results. In the QG momentum equations (2.14) and (2.15), we substitute $u_g = \bar{u}_g + u_g'$ and $v_g = v_g'$, noting that $\bar{u}_g$ is a function only of the y and z directions, and then we take the scalar product with $\vec{V}_g'$ and rearrange to yield

$$\frac{\partial}{\partial t}\left(\frac{u_g'^2 + v_g'^2}{2}\right) + u_g\frac{\partial}{\partial x}\left(\frac{u_g'^2 + v_g'^2}{2}\right) + v_g\frac{\partial}{\partial y}\left(\frac{u_g'^2 + v_g'^2}{2}\right)$$
$$= f(u_g' v_{ag} - v_g' u_{ag}) - u_g' v_g' \frac{\partial \bar{u}_g}{\partial y}. \tag{2.42}$$

Combining the left-hand terms, substituting the perturbation geostrophic wind definitions $v_g' = (1/f)\partial\phi'/\partial x$ and $u_g' = -(1/f)\partial\phi'/\partial y$ in the rightmost term, and using the product rule of calculus, the equation

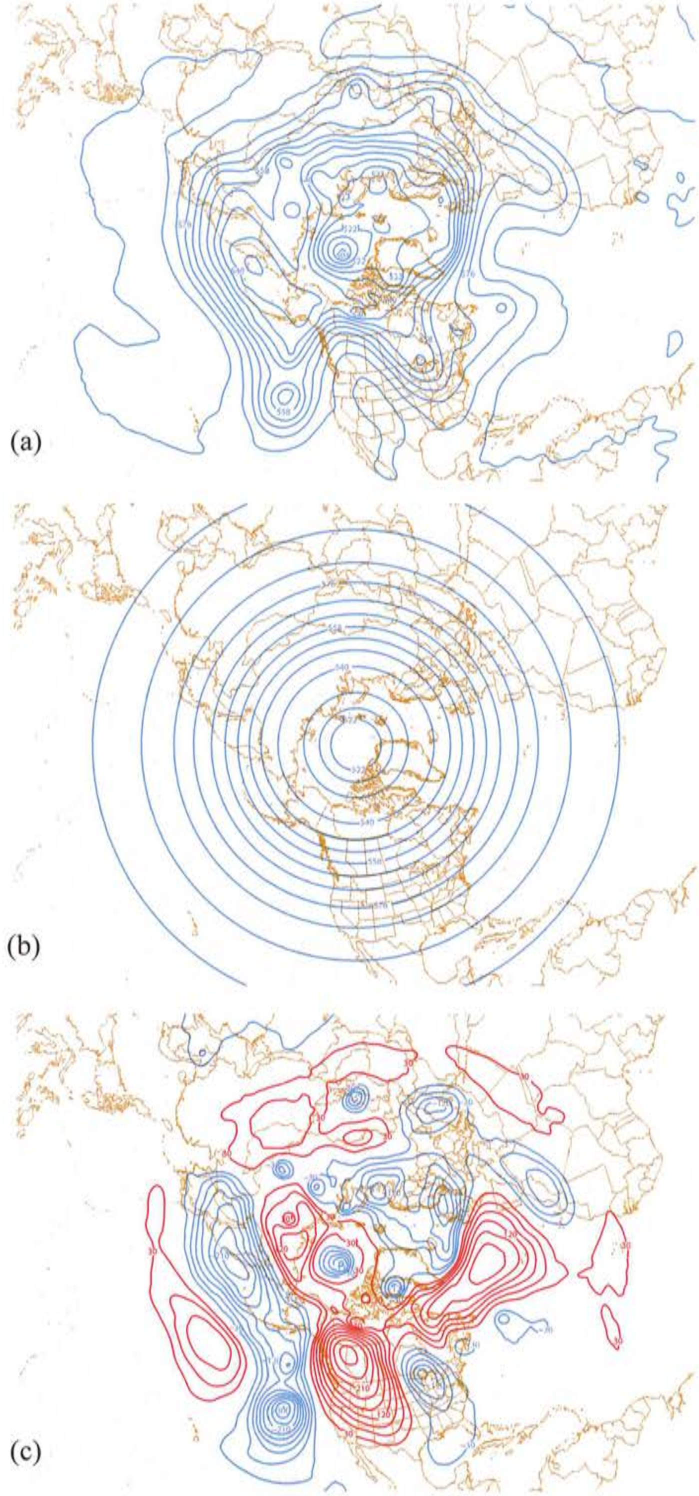

Figure 2.18. Decomposition of 500-mb geopotential height derived from GFS analysis valid 1200 UTC 30 Sep 2008: (a) full height field, contour interval is 6 dam; (b) zonal average height; and (c) height anomaly, interval 30 m, blue (red) lines represent negative (positive) anomaly values. The zero contour is omitted.

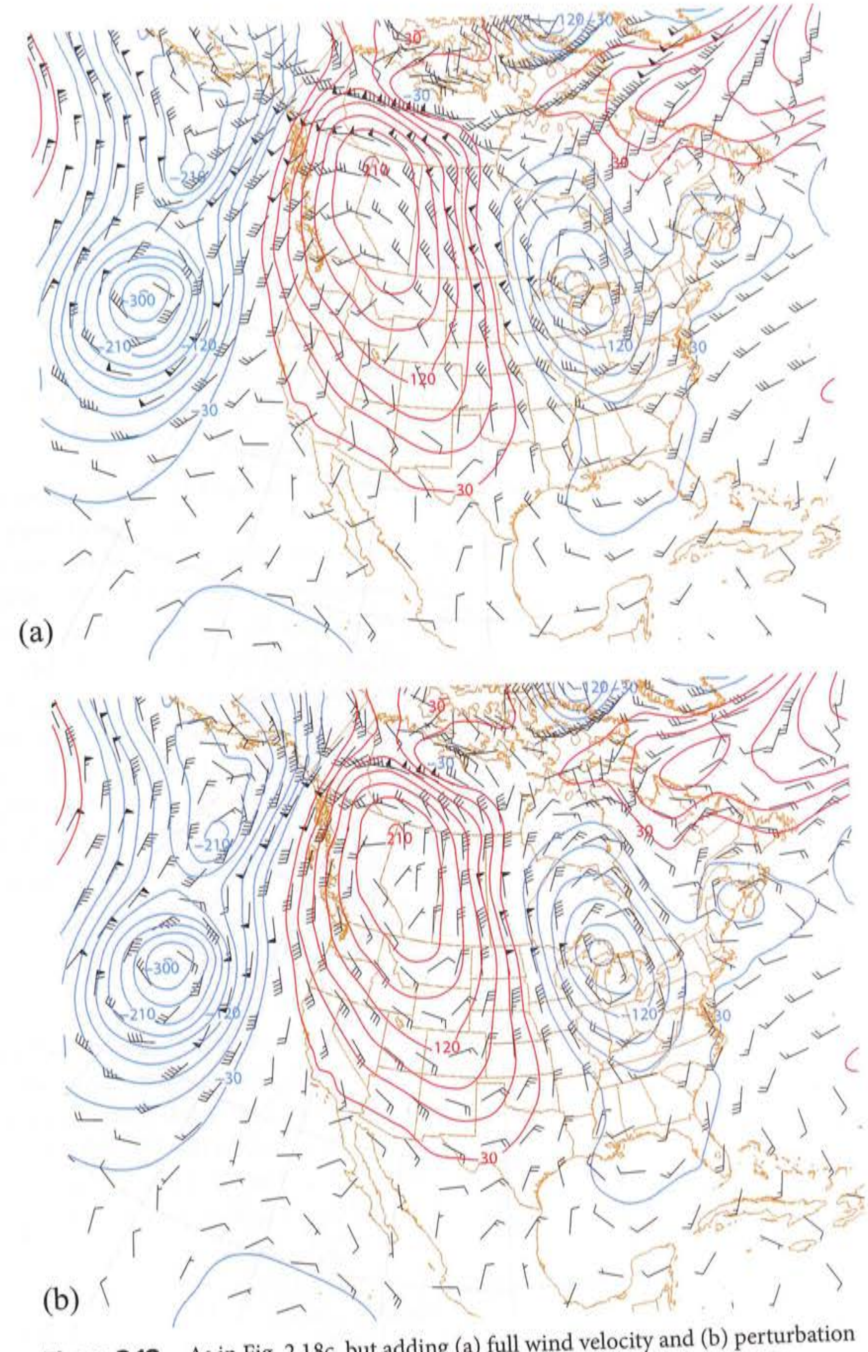

Figure 2.19. As in Fig. 2.18c, but adding (a) full wind velocity and (b) perturbation velocity. Winds are plotted as barbs using standard plotting convention.

takes the following form (the complete derivation is assigned as an end-of-chapter problem):

$$\frac{d}{dt_g}\left(\frac{u_g'^2+v_g'^2}{2}\right) = -\nabla\cdot(\phi'\vec{U}_{ag}) - \frac{R_d}{g\,p}\omega'T' - u_g'\,v_g'\,\frac{\partial \bar{u}_g}{\partial y}. \tag{2.43}$$

This equation is useful for the quantification of local energetics and can be applied in a variety of contexts. The left-hand side describes changes in K_{eg} following the geostrophic flow, or we can split this into local and advective tendencies. The right-hand terms represent the *ageostrophic geopotential flux divergence*, *baroclinic conversion*,

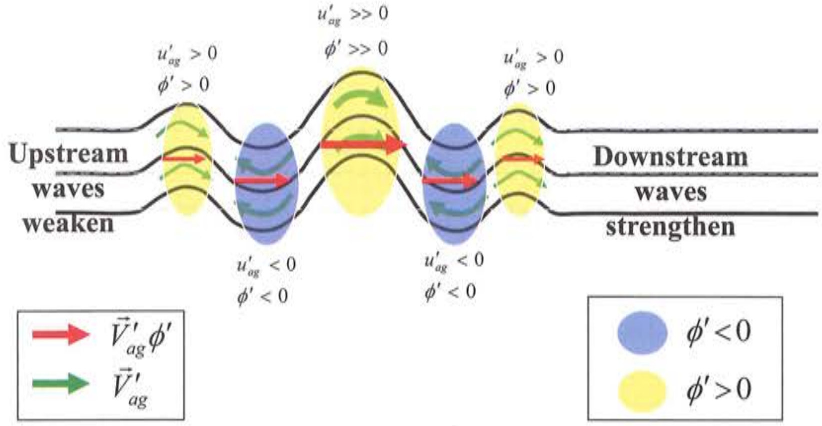

Figure 2.20. Illustration of ageostrophic geopotential flux in downstream baroclinic development. Solid black lines represent geopotential height contours; shaded yellow and blue ovals represent height anomalies of positive and negative sign, respectively; green curved arrows represent sense of horizontal ageostrophic flow; and red arrows depict the ageostrophic geopotential flux.

and *barotropic conversion*, respectively. We will explore these three terms in more detail below.

In chapter 1, we noted that the *group velocity* for Rossby wave energy exhibited a faster eastward movement than the speed of individual troughs and ridges, evident, for example, in Fig. 1.20. The eastward propagation of wave energy is described by the first right-hand term in (2.43), the divergence of the ageostrophic geopotential flux, as illustrated in Fig. 2.20. Because this term is related to the product of the ageostrophic velocity vector and the geopotential anomaly, the flux has an eastward-directed zonal component throughout a train of Rossby waves. This is because in locations where the flow is subgeostrophic (in troughs, providing a negative ageostrophic zonal wind component there), the geopotential anomaly is also negative, providing a positive (eastward)-directed flux; in ridges, both terms are positive. The result is an eastward-directed flux of Rossby wave energy. For a wave train without spatial variations in wave amplitude, the eastward flux is uniform across the troughs and ridges, and the flux divergence is zero. However, the atmosphere typically exhibits regions of highly amplified troughs and ridges, with regions of weak wave amplitude upstream and downstream. In this situation, similar to that shown in Fig. 2.20, there will be *energy flux convergence* downstream of the region of large-amplitude waves, and the wave amplitudes will tend to grow there. Meanwhile, the energy flux divergence upstream will result in weakening waves there. Orlanski and Katzfey (1991) and Orlanski and Chang (1993) have shown that the downstream energy flux associated with this process is a major factor in the amplification and decay of many upper-level disturbances.

An example of this, taken from a typical situation over North America, is provided in Fig. 2.21. Amplified upper waves are observed over the North Pacific and western North America at the initial time (Figs. 2.21a,b). These panels demonstrate the supergeostrophic (subgeostrophic) nature of the flow in the ridge (trough) and also the pattern of ageostrophic geopotential flux. Thus, Rossby wave energy is moving eastward, and we expect the upstream height anomalies to decay while the eastern anomalies amplify (including the trough over the central United States). The amplified trough over eastern North America evident in Fig. 2.21c is consistent with expectations based on the idealized schematic (Fig. 2.20).

Interpretation of the barotropic and baroclinic terms in (2.43) is facilitated by utilizing an average over a specified domain of interest. With suitable lateral boundary conditions, such as a periodic domain in the x direction and a bounded domain in the y direction, we can average over the depth of the troposphere and a horizontal area A to obtain an integral form of the eddy kinetic energy equation

$$\underbrace{\frac{\partial [K_{eg}]}{\partial t}}_{A} = \underbrace{-\frac{1}{gA}\int_p\int_A \overline{u'_g v'_g}\,\frac{\partial \overline{u}_g}{\partial y}\,dA\,dp}_{B} + \underbrace{\frac{R_d}{A}[\rho]\int_p\int_A \overline{w'T'}\,dA\,d\ln p}_{C}. \qquad (2.44)$$

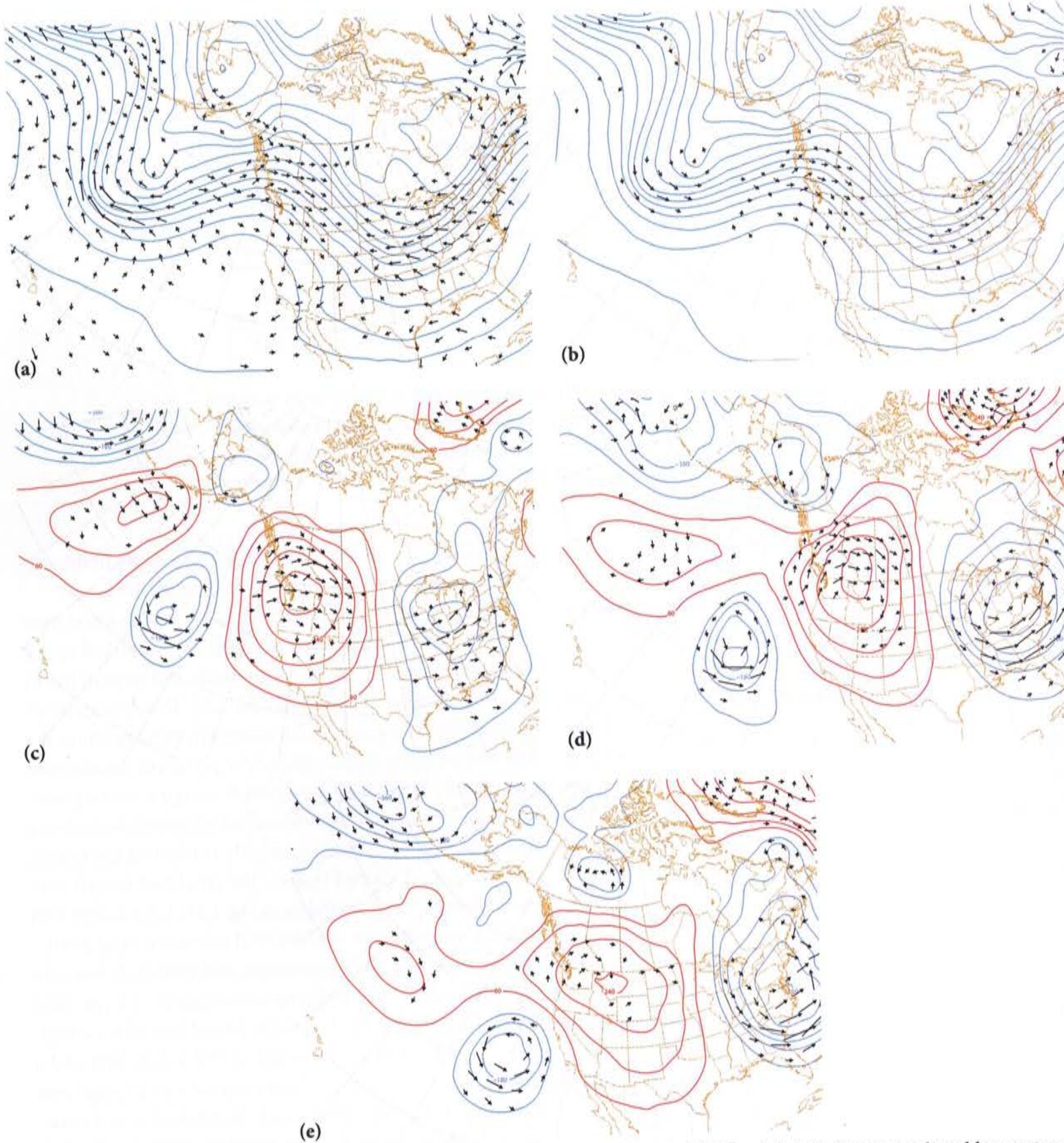

Figure 2.21. Example of downstream development for 0000 UTC 2 Feb 2009: (a) 500-mb height (interval 6 dam, blue contours) and ageostrophic wind vectors; (b) as in (a) but with ageostrophic geopotential flux (vectors); (c) 500-mb height anomaly (interval 60 m, zero contour omitted), positive (negative) anomalies red (blue) contours valid 0000 UTC 3 Feb 2009; (d) as in (c) except for 0000 UTC 4 Feb; (e) as in (c) except for 0000 UTC 5 Feb. Vectors in (c)–(e) are as in (b).

For example, the domain could be taken as a latitudinal belt encircling the globe, consistent with periodic boundary conditions in the zonal direction. Because the advection and ageostrophic geopotential flux redistribute eddy energy within such a domain, these terms do not appear in the volume-averaged version of the equation. Cyclones and anticyclones can be viewed as "eddies" in a background flow that is more or less zonal. Equation (2.44) tells us what processes and mechanisms determine whether the energy in such a disturbance will grow or diminish with time. The energetics framework can also be used in diagnosing the role that eddy disturbances play in the global energy balance. The left side of (2.44), term A, is simply the local time rate of change in eddy kinetic energy, averaged over the entire area and depth of a given domain or disturbance. This term will be positive for an eddy disturbance, such as a cyclone or anticyclone, that is growing in amplitude.

Inspection of the first right-hand term (term B) reveals a dependence on the meridional gradient of the zonal-mean flow, $\partial \bar{u}_g / \partial y$, and the spatial average of the perturbation velocity product $\overline{u'_g v'_g}$. The former will be largest in magnitude in regions where there is strong meridional shear of the mean flow, and it will be very small near the axis of the zonally averaged jet. The eddy product term $\overline{u'_g v'_g}$ requires more analysis. Considering this quantity for a perfectly circular eddy, as depicted in Fig. 2.22, we find that there is cancellation between this product in different parts of the eddy, and the average over the entire eddy is zero. The area-averaged eddy velocity product also equals zero for elongated eddies that do not have a pronounced axial tilt.

Consider now an asymmetric eddy with an axial tilt, as shown in Fig. 2.23. We see that when averaged around the circumference of the disturbance, there is a disproportionate region that is characterized by *negative*

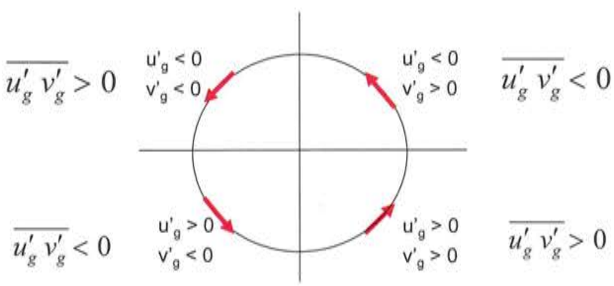

Figure 2.22. Eddy flow correlations for a circular eddy disturbance.

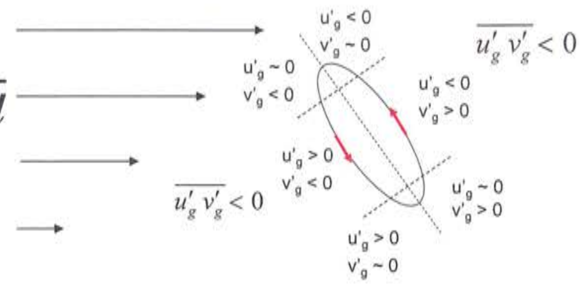

Figure 2.23. As in Fig. 2.22, but for an asymmetric eddy with a tilted axis. Arrows at left depict mean zonal flow.

values of $\overline{u'_g v'_g}$. For such "negatively tilted" eddies in the Northern Hemisphere, if located south of the region of strongest westerly $\bar{u}_g$ in the region where $\partial \bar{u}_g / \partial y > 0$, then a positive contribution to the eddy kinetic energy arises because of term B in (2.44). The physical process at work is related to the extraction of kinetic energy from the zonal mean flow, into the eddy, and it takes place with an axis oriented so that the eddy is *leaning against the background shear*. In many physical systems, this characteristic is associated with the growth of eddy energy at the expense of the reservoir of mean flow kinetic energy. To draw a loose analogy, imagine a stream or river with the strongest average flow in the center, weakening toward either bank. If one were to insert a barrier (e.g., a piece of plywood) into the flow oriented in a way that cut against the shear of the river current, then one can imagine a whirlpool (eddy) forming because of the extraction of energy from the mean current into the eddy. This is by no means an exact physical analog to what happens in the atmosphere, however, because the sense of the flow would only support an eddy with one sense of rotation for a given side of the river, whereas rotation in either sense is supported by term B.

Analysis of the barotropic energy conversion term provides useful information concerning the nature of trough and ridge structures and their potential for growth through this mechanism. For symmetric disturbances, or those centered near the mean jet core, this mechanism will not be important. In regions with strong shear of the mean zonal flow, however, it can be important for strongly tilted eddies. For Northern Hemisphere locations on the equatorward side of the mean jet core, a "negatively tilted trough" is a configuration favorable for barotropic energy growth, while positively tilted troughs lose energy to the mean flow through this mechanism. This terminology is

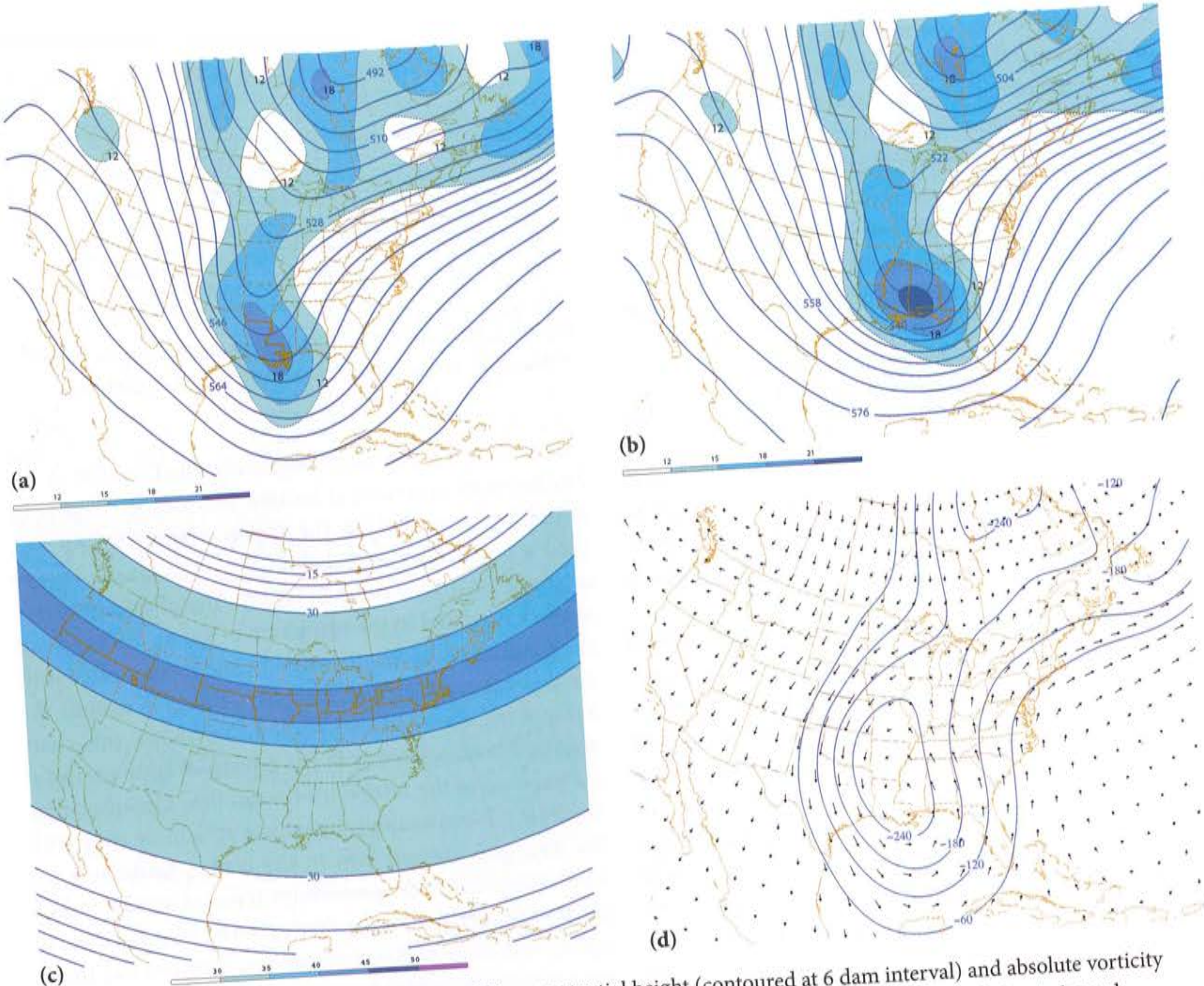

Figure 2.24. 500-mb level plots for 13 Mar 1993: geopotential height (contoured at 6 dam interval) and absolute vorticity (shaded as in legend) at (a) 0600 and (b) 1200 UTC; (c) zonal average of zonal wind contoured and shaded as in legend; and (d) 500-mb negative height anomaly (interval 60 m) and wind anomalies.

consistent with the sense of progression of the trough axis with increasing latitude; for example, a positively tilted trough exhibits an axis that is displaced in the positive x direction with increasing y.

A classic example of a negatively tilted trough south of the mean jet core took place on 12–14 March 1993 in the so-called Storm of the Century in the eastern U.S. Several processes were at work to produce the highly amplified trough evident in Figs. 2.24a,b; however, one mechanism of potential importance was the barotropic kinetic energy conversion process. This trough is negatively tilted, and Fig. 2.24c confirms that $\partial \bar{u}_g / \partial y$ is positive in the region of negative trough axis tilt, ensuring that the sign of the barotropic term is positive for this system. It would require a careful computation of the entire energy budget to quantify the importance of this process in this storm; nevertheless, there is sufficient circumstantial evidence here for a forecaster to note this aspect and consider that this process would favor kinetic energy growth for the upper trough system.

Some words of caution are in order—First, not all negatively tilted troughs strengthen because of barotropic energy conversion! For instance, near the latitude of the mean jet core, where $\partial \bar{u}_g / \partial y \sim 0$, this term is negligible. Second, north of the jet core where $\partial \bar{u}_g / \partial y < 0$, a negatively tilted trough will result in the **weakening** of kinetic energy because of the barotropic conversion process. The need to compute $\partial \bar{u}_g / \partial y$ is somewhat cumbersome, but

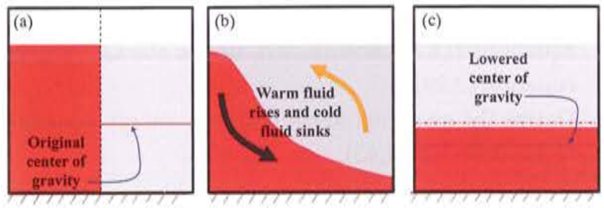

Figure 2.25. Schematic depiction of baroclinic energy conversion process. (a) System contains available potential energy; dashed line indicates a barrier separating dense (red) fluid and lighter (gray) fluid. (b) Once barrier is removed, dense fluid sinks and lighter fluid rises; kinetic energy is generated as potential energy is released. (c) In the final state, the center of gravity of system has been lowered, and a net loss of potential energy has occurred (adapted from Carlson 1998).

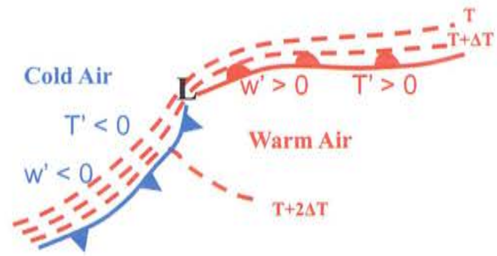

Figure 2.26. Schematic of baroclinic energy conversion in an idealized extratropical cyclone. Dashed lines represent isotherms, and the sign of temperature anomalies and vertical motions are indicated in select locations.

it is easily done using standard meteorological software packages. The main point of this analysis is that the structure of upper troughs and ridges is important to their energy growth or decay. Other aspects affected by these structural properties include the ability of such systems to transport momentum horizontally, as a part of the planetary-scale circulation.

The remaining right-hand term in (2.44), term C, is proportional to the correlation between the vertical motion and the temperature anomaly, averaged over the volume in question. This term represents the vertical heat flux. Unlike the barotropic conversion term, which describes the conversion of *existing* kinetic energy from the mean into the eddy flow, this term describes the *generation* of kinetic energy resulting from the conversion from potential energy, known as *baroclinic* energy conversion.

When, on average within a weather system, warm air rises and cold air sinks, this term contributes positively to the eddy kinetic energy through the conversion of potential to kinetic energy in the system. A visual analog is provided in Fig. 2.25, in which a container initially contains two fluids of different density, separated by a divider. At this initial time, because some of the dense fluid (left side in Fig. 2.25a) is located above less dense fluid (right side), there is *available potential energy* in the system that can be converted to kinetic energy. If the divider is removed, kinetic energy is generated as the dense fluid flows beneath the lighter fluid; potential energy is converted to kinetic energy at this stage (Fig. 2.25b). In the end after friction has eliminated the motion, the center of gravity of the system has lowered, and available potential energy has been converted to kinetic energy and then dissipated as thermal energy by friction (Fig. 2.25c).

If we carry this simple analogy over to a typical midlatitude cyclonic weather system, then it is clear that on average, air in regions of the system characterized by anomalous warmth (e.g., relative to a latitudinal average) is rising while anomalously cold air is sinking (Fig. 2.26). This is also related to the tendency for warm advection (cold advection) to be associated with forcing for ascent (descent), as evident from the QG omega equation; on average, there is conversion of potential to kinetic energy in a developing cyclone with this type of thermal pattern.

There are a number of useful insights offered by the consideration of baroclinic energy conversion. First, in general, the stronger the thermal contrast in the vicinity of a cyclonic system, the stronger the magnitude of the thermal advection pattern, and thus both factors in this term are maximized. Therefore, we expect that strongly developing cyclonic systems are characterized by large temperature contrasts, a finding that is entirely consistent with observation. Second, this explains the seasonality of cyclones—in the summer with generally reduced horizontal thermal contrasts, the baroclinic energy conversion term is weakened. In our discussion of cyclones in chapter 5, we will return to these arguments to explain some aspects of the observed cyclogenesis distribution.

REVIEW AND STUDY QUESTIONS

1. Some of the assumptions used in the derivation of the QG omega and height tendency equations are questionable for midlatitude synoptic-scale cyclones. Discuss two of the most limiting assumptions, and